cervical spine and spinal canal.[9–11] To evaluate the dynamic factors in patients with CSM, several authors have reported that kinematic MRI is a useful modality that demonstrates physiological alterations of the spinal canal and spinal cord in different neck positions (flexion-extension).[12–14]

Recently, other studies have shown the efficacy of kinematic CT myelography to investigate dynamic factors in patients with CSM.[15,16] The authors evaluated the dynamic changes in spinal cord compression using reconstructed images obtained with multidetector-row CT after myelography. In comparison with kinematic MRI, kinematic CT myelography offers several advantages, including a shorter scanning time, thinner axial slices, and high image resolution, particularly in bony or calcified compressive lesions.[15,16] However, to our knowledge, no studies have evaluated dynamic factors in patients with OPLL using kinematic CT myelography.

The decision to choose surgical intervention for patients with cervical myelopathy is based on the appropriate clinical diagnosis and confirmation at imaging studies. It is known that the amount of spinal cord compression can change depending on the neck position.[3,17] Therefore, the dynamic imaging study can provide important information to make a treatment decision. In this study, we investigated the dynamic changes in spinal cord compression in patients with myelopathy caused by cervical OPLL using reconstructed kinematic CT myelography images.

MATERIALS AND METHODS

From April 2008 to April 2013, 51 consecutive patients with OPLL who presented with myelopathy secondary to OPLL were prospectively enrolled in this single-institution study. In this study, spondylosis without OPLL, trauma, infection, calcification of ligamentum flavum, tumor, and cases with a history of previous cervical spine surgery were excluded. The patients' neurological condition was assessed using the Japanese Orthopaedic Association (JOA) score.[18] Cervical plain radiographs and MRI images were obtained in a neutral position before admission. Ossification types determined by lateral radiograph were classified as continuous, segmental, mixed, and other according to the criteria proposed by the Investigation Committee on the Ossification of Spinal Ligaments of the Japanese Ministry of Public Health and Welfare.[19,20] The level of the greatest spinal cord compression by OPLL was determined using the midsagittal images of the neutral MRI. The occupying rate of OPLL at the most compressed level was calculated as the thickness of the OPLL/anterior-posterior (A-P) diameter of the spinal canal ×100 (%) using lateral radiograph.[21] This study was approved by an institutional review board.

Kinematic CT Myelography

The examinations were performed under supervision of 4 spine specialists. After 15 mL of the contrast medium iohexol (Omnipaque, Daiichi Pharmaceutical Co., Tokyo) was injected into the lumbar cerebrospinal fluid space, a dynamic motion study was performed using multidetector CT (Aquilion64, TOSHIBA Medical System Inc., Tokyo). The CT images were obtained in both the neck flexion and extension positions to the greatest extent possible, as limited by the patients. The scanning parameters were as follows: 120 kV, 100 to 300 mA, 0.5-mm thickness for slice data, and 0.5 mm thickness for reconstruction. The scanning time for the cervical spine in each position was less than 10 seconds. No patients displayed neurological deterioration during the kinematic CT examinations.

Evaluation

Using the reconstructed CT images obtained with this method, the range of motion (ROM) at C2–C7 from flexion to extension was evaluated in the midsagittal view by measuring the angle between the lower endplate of the C2 and C7 vertebrae. The segmental ROM was measured in the same fashion between the lower endplates of the upper and lower vertebrae at the level where the spinal cord was most compressed by OPLL. The A-P diameter of the spinal cord was measured in the midsagittal view at the level of the greatest spinal cord compression by OPLL (Figure 1A). Additionally, the cross-sectional area (CSA) of the spinal cord was measured in the axial view at the most compressed level using image analysis software (Figure 1B; ImageJ: NIH, Bethesda, MD). We evaluated the dynamic changes in the A-P diameter and the CSA of the spinal cord and defined their rate based on the following formula: the A-P diameter (or CSA) in flexion/the A-P diameter (or CSA) in extension. The data were collected prospectively. The paired *t* test and Pearson correlation test were used for statistical analysis. *P* values less than 0.05 were considered significant.

RESULTS

The study included 39 males and 12 females (63.5 ± 8.7 yr old, range: 40–79). There were 18 patients with segmental-type OPLL, 33 patients with mixed-type OPLL, and no patients with the continuous type. The JOA score for the

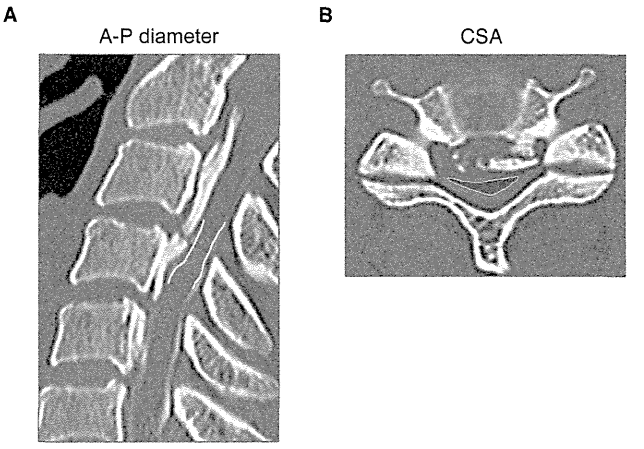

Figure 1. A, The A-P diameter of the spinal cord measured in the midsagittal view at the level of the greatest spinal cord compression by OPLL. **B**, The CSA of the spinal cord was measured in the axial view at the most compressed level. OPLL indicates ossification of the posterior longitudinal ligament; A-P, anterior-posterior; CSA, cross-sectional area.

patients' neurological condition was 10.8 ± 2.4 points (4.5–14.5 points). The level of the greatest spinal cord compression by OPLL was C2–C3 in 2 patients, C3–C4 in 18 patients, C4–C5 in 11 patients, C5–C6 in 15 patients, and C6–C7 in 5 patients. The occupying rate of OPLL at the most compressed level was 47.1 ± 12.7% (Table 1).

In the kinematic CT myelography, the mean ROM at C2–C7 from flexion to extension was 23.1 ± 11.7°. The segments of the greatest spinal cord compression of all patients included in this study were mobile without complete bridging of OPLL between the upper and lower vertebrae. The segmental ROM at the most compressed level was 7.0 ± 4.4° (Table 2).

The A-P diameters of the spinal cord at the most compressed levels were significantly decreased during neck extension compared with neck flexion ($P < 0.01$; Figure 2A, B). The spinal cord was more compressed by the OPLL during neck extension in 86.3% (44/51) of the patients (Figure 2A; Table 2). Similarly, the CSAs at the most compressed levels were also significantly decreased during neck extension when compared with flexion ($P < 0.01$; Figure 3A, B). The CSAs were decreased during neck extension in 86.3% (44/51) of the patients (Figure 3A; Table 2). We also evaluated the correlation between the severity of the neurological impairment and the dynamic change of the A-P diameter and CSA of the spinal cord (the difference between flexion and extension). However, no significant correlation was found between the dynamic change and the JOA neurological score ($P > 0.05$).

TABLE 1. Patients' Data

N	51
Age (yr)	63.5 ± 8.7 (range: 40–79)
Male/female	39/12
Types of OPLL	
Segmental type	18
Mixed type	33
Continuous type	0
JOA neurological score (/17 points)	10.8 ± 2.4 (range: 4.5–14.5)
Level of the greatest spinal cord compression	
C2–C3	2
C3–C4	18
C4–C5	11
C5–C6	15
C6–C7	5
Occupying rate of OPLL (%)	47.1 ± 12.7

Types of OPLL were classified using lateral radiograph.[19,20] Neurological dysfunction was assessed using JOA score for the cervical spine.[18] The occupying rate of OPLL was calculated as the thickness of the OPLL/anterior-posterior diameter of the spinal canal × 100 (%) using lateral radiograph.[21]

OPLL indicates ossification of the posterior longitudinal ligament; JOA, Japanese Orthopaedic Association.

TABLE 2. Kinematic CT Myelography

	Flexion	Extension
Lordosis at C2–C7 (°)	−6.1 ± 11.0	17.4 ± 11.5
ROM at C2–C7 (°)	23.1 ± 11.7	
Lordosis at the greatest compressed level (°)	−2.8 ± 6.1	4.1 ± 5.8
ROM at the greatest compressed level (°)	7.0 ± 4.4	
A-P diameter of spinal cord (mm)	3.4 ± 1.3*	3.0 ± 1.2
No. of patients with increased spinal compression		
Occupying ratio ≥60% (N = 11)	7	4
Occupying ratio <60% (N = 40)	0	40
CSA of spinal cord (mm²)	39.3 ± 10.5*	34.3 ± 10.3
No. of patients with increased spinal compression		
Occupying ratio ≥60% (N = 11)	7	4
Occupying ratio <60% (N = 40)	0	40

**P < 0.01.*

ROM indicates range of motion; A-P diameter, anterior-posterior diameter of spinal cord at the greatest compressed level in the midsagittal view; CSA, cross-sectional area of the spinal cord at the greatest compressed level in the axial view.

Although the compression of the spinal cord was increased in most of the patients in this study (Figure 4A), the A-P diameter and the CSA of the spinal cord were decreased during neck flexion in 13.7% (7/51) of the patients (Figure 4B; Table 2). Notably, all 7 of these patients had massive OPLL, with a 60% or more occupying rate (an average of 64.3 ± 5.0%), which was significantly higher than the rate in the other 44 patients (44.3 ± 11.3%). Furthermore, we compared the

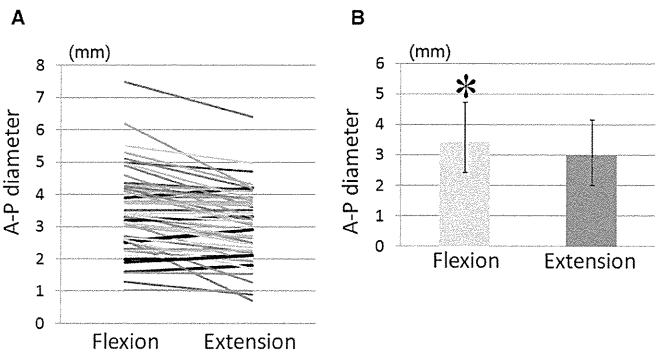

Figure 2. A, The dynamic changes in anterior-posterior diameter of the spinal cord (from flexion to extension). The black lines: patients with the greater spinal cord compression during neck flexion. **B**, The A-P diameter of the spinal cord at the level of the greatest spinal cord compression was significantly decreased during neck extension when compared with neck flexion (*$P < 0.01$). A-P indicates anterior-posterior.

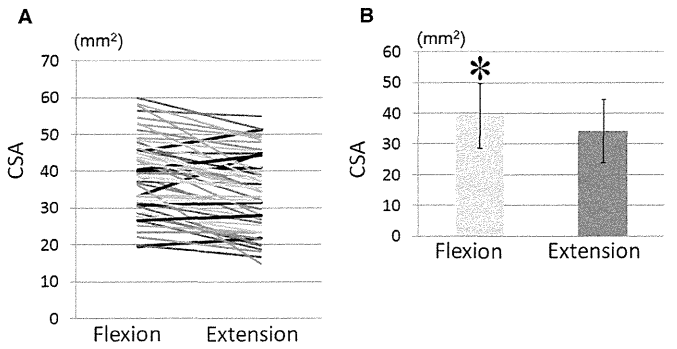

Figure 3. **A**, The dynamic changes in CSA of the spinal cord (from flexion to extension). The black lines indicate patients with the greater spinal cord compression during neck flexion. **B**, The CSA of the spinal cord at the most compressed level was significantly decreased during neck extension when compared with neck flexion (*$P < 0.01$). CSA indicates cross-sectional area.

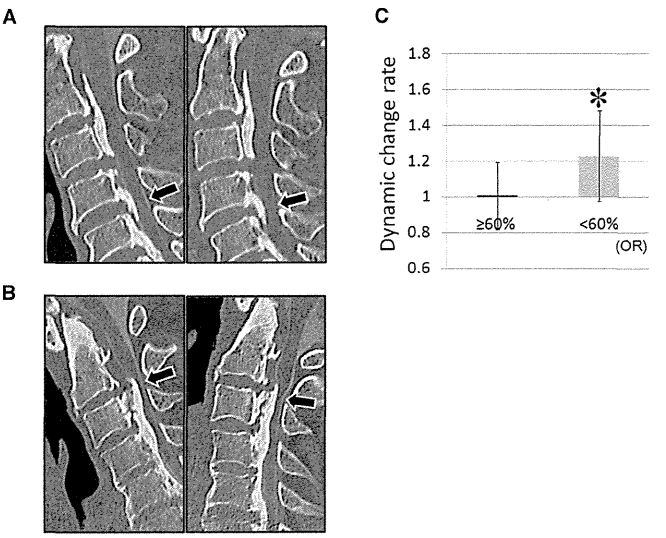

Figure 4. **A**, A case of increased spinal cord compression in neck extension. **B**, A case of increased spinal cord compression in neck flexion. The black arrows indicate the levels where the spinal cord was most compressed by OPLL. **C**, The dynamic change rate of CSA of the spinal cord (flexion/extension): patients with OPLL OR ≥ 60% *vs.* patients with OR < 60% (*$P < 0.05$). OPLL indicates ossification of the posterior longitudinal ligament; CSA, cross-sectional area; OR, occupying rate.

dynamic change rate of the A-P diameter and CSA (flexion/extension) between the subgroups: patients with a 60% or more OPLL occupying rate *versus* those with less than 60% OPLL. The dynamic change rate was significantly lower in patients with an OPLL occupying rate 60% or more ($P < 0.05$) (Figure 4C), suggesting that severe spinal cord compression during neck flexion tends to occur more frequently in patients with massive OPLL.

We further compared the different types of OPLL: segmental type and mixed type (Table 3). The proportion of males was higher in the mixed type of OPLL. Although the age and JOA neurological score were similar in the both types, the occupying rate was significantly higher in the mixed type ($P < 0.05$). In the kinematic CT myelography, the ROM at C2–C7 and at the level with greatest spinal cord compression tended to be higher in the segmental type; however, significant differences were not found. The A-P diameter and CSA of the spinal cord were significantly decreased during neck extension in both the segmental and mixed types. However, the increased spinal cord compression during neck flexion was more frequently observed in the mixed type OPLL (6/33 cases: 18.2%) than in the segmental type (1/18 cases: 5.6%).

DISCUSSION

This study prospectively investigated 51 patients with OPLL with relatively severe myelopathy (average JOA score: 10.8 points) using kinematic CT myelography. In all of the included patients, the OPLL was segmental type or mixed type, and the segments with the greatest spinal cord compression were mobile, with an average ROM of 7.0°. Static spinal cord compression is known to be an important factor in the development of myelopathy caused by OPLL, including the occupying rate of OPLL and the residual space for the spinal cord.[22–25] Matsunaga *et al*[24] reported that patients developed myelopathy at high rates when the space available for the spinal cord was less than 6 mm, whereas the patients with the space available for the spinal cord 14 mm or more did not. Dynamic factors are also important in the mechanism of neurological symptoms in OPLL.[6,7,24] A cadaveric study conducted by Inufusa *et al*[3] showed that the spinal canal area changed more than 20% by neck motion (flexion-extension). Furthermore, a larger ROM of the cervical spine is associated with the development of myelopathy,[24] whereas symptomatic myelopathy does not often develop when the ROM of the cervical spine is highly restricted by continuous OPLL.[26] As Azuma *et al*[6] have previously reported, both static cord compression and dynamic factors have an important role in the pathogenesis of myelopathy.

In this study, we used kinematic CT myelography for the evaluation of dynamic changes in spinal cord compression caused by OPLL. MRI is the most universally used diagnostic tool for investigating cervical myelopathy.[11] Previous reports have described the efficacy of functional studies using MRI to evaluate dynamic factors in patients with cervical myelopathy.[12–14] However, it is difficult to precisely assess the spinal cord CSA during flexion and extension because of image resolution limitations in MRI. Conventional myelography can offer a dynamic evaluation of the cervical spine. However, it is difficult to obtain sufficient information to evaluate the dynamic changes precisely in spinal cord compression because conventional myelography lacks axial images.

Recent studies have shown the usefulness of kinematic CT myelography to investigate the contributions of dynamic factors to the development of myelopathy in patients with CSM.[15,16] Machino *et al*[15] has shown that the spinal cord CSA is significantly decreased during neck extension at each level of the cervical spine. Although CT myelography requires a dural puncture and radiation exposure, high-resolution multidetector CT offers some advantages. The use of multidetector CT after myelography provides clearly contrasted

TABLE 3. Comparison of Different Types of OPLL

	Segmental Type	Mixed Type
N	18	33
Age (yr)	65.6 ± 7.5	63.2 ± 9.1
Male/female	12/6	27/6
JOA neurological score (/17 points)	10.9 ± 2.3	10.8 ± 2.4
Occupying rate of OPLL (%)	40.1 ± 12.4	50.8 ± 11.4*
ROM at C2–C7 (°)	26.0 ± 11.1	21.6 ± 11.9
ROM at the greatest compressed level (°)	7.6 ± 3.7	6.6 ± 4.8
A-P diameter of spinal cord		
Flexion-extension (mm)	4.0 ± 1.5†/3.3 ± 1.5	3.1 ± 1.0†/2.9 ± 0.9
No. of patients with increased spinal compression (during flexion/during extension)	1/17	6/27
CSA of spinal cord		
Flexion-extension (mm^2)	39.9 ± 11.2†/34.2 ±11.8	38.9 ± 10.4†/34.4 ± 9.6
No. of patients with increased spinal compression (during flexion/during extension)	1/17	6/27

**P < 0.05 (segmental vs. mixed).*

†P < 0.05 (flexion vs. extension).

OPLL indicates ossification of the posterior longitudinal ligament; ROM, range of motion; A-P diameter, anterior-posterior diameter of spinal cord at the greatest compressed level in the midsagittal view; CSA, cross-sectional area of the spinal cord at the greatest compressed level in the axial view; JOA, Japanese Orthopaedic Association.

images of the vertebrae, spinal cord, cerebrospinal fluid space, and compressive factors in axial and sagittal reconstructed slices. CT myelography is particularly useful for evaluating the bony compressive focus in such disorders as OPLL. In addition, there is less possibility for neurological deterioration during the examination because the scanning time is short. Indeed, in the patients examined using kinematic CT myelography in this study, we did not observe any symptom deterioration.

In this investigation of dynamic factors in patients with OPLL using kinematic CT myelography, spinal cord compression was significantly increased during neck extension in both the segmental and mixed-type OPLL. The amount of the dynamic change in spinal cord compression did not show significant correlation with the neurological scores, because various factors influence the severity of the neurological dysfunction.[2,27,28] However, as shown in several studies, increased spinal cord compression during neck extension is known as a common dynamic factor in patients with cervical myelopathy.[12,13,15,16] During neck extension, both anterior (*e.g.*, OPLL) and posterior factors (*e.g.*, buckling of the ligamentum flavum) contribute to increased spinal cord compression (pincer effect).[14,17] We sometimes encounter patients with OPLL with progressive myelopathy whose spinal cord compression is mild in a neutral position. The dynamic imaging study is considered useful for evaluating such patients. It has also been reported that the number of levels of spinal cord compression can be increased during neck extension compared with the neutral position.[16] Therefore, kinematic CT myelography can provide critical information for determining the number of levels that should be treated during surgery.

Although spinal cord compression was increased during neck extension in most of the patients with OPLL, greater amounts of compression may be placed on the spinal cord during neck flexion in patients having OPLL with a high occupying rate. In this study, increased cord compression during neck flexion was found in 7 of the 51 (13.7%) patients. The rate of increased compression during neck flexion in patients with OPLL seems to be higher than that in patients with CSM (3%–5%).[12,14] Interestingly, all 7 of these patients had massive OPLL with an occupying rate 60% or more. In addition, the OPLL occupying rate in the patients with increased cord compression during neck flexion was significantly higher than other patients. In comparison of different types of OPLL, the occupying rate was significantly higher in the mixed-type OPLL; thus the severe spinal cord compression during neck flexion occurred more frequently in patients with mixed-type OPLL. In patients with massive OPLL, the anterior factor (*i.e.*, OPLL) is considered to influence the pathogenesis of increased compression during neck flexion more significantly than the posterior factor.[14] Posterior laminoplasty is often used to treat OPLL in clinical settings,[8,29,30] and it is usually performed under neck flexion because the spinal cord is more easily and safely decompressed during neck flexion in most

patients. However, care should be taken during surgery to avoid excessive neck flexion, which can increase spinal cord compression and possibly cause intraoperative neural injury in patients with massive OPLL.[31]

Previous studies have reported that the surgical outcome after posterior decompression (*i.e.*, laminoplasty) tends to be insufficient in patients with OPLL with a large occupying rate.[21,24,25,32] Several authors demonstrated that the occupying rate (≥60% or <60%) was clinically important to determine the surgical procedure (anterior or posterior).[24,32] Therefore, we focused on the occupying rate of OPLL and used 60% as the cutoff point in this study. As this study shows, patients with massive OPLL can experience severe spinal cord compression even in the neck flexion position; in these cases, the anterior factor is a major cause of compression. Surgically treating patients with massive OPLL with posterior decompression, which only removes the posterior elements, can result in residual dynamic spinal cord compression by OPLL during neck flexion.[17] As previously reported, direct decompression through an anterior approach or posterior decompression with fusion may lead to better neurological recovery for patients with OPLL with a high occupying rate.[7,21]

We note some limitations of this study. Kinematic CT myelography has some drawbacks; in particular, the use of contrast medium and radiation exposure carry the risk of adverse effects for patients. However, the high-resolution images and the low risk of neurological deterioration during examination are great merits of kinematic CT myelography. In this study, the kinematic studies were performed only during neck flexion and extension and not at the neutral position. Examinations in 3 different positions may show interesting patterns of dynamic changes in spinal cord compression; however, increasing the number of positions for examination further increases patients' risk of radiation exposure. Despite these limitations, kinematic CT myelography was useful for evaluating the dynamic causative factors in the pathogenesis of myelopathy induced by OPLL, and it provided high-quality functional images without any neurological deterioration during the examinations.

CONCLUSION

We evaluated patients with OPLL with myelopathy using kinematic CT myelography. This functional study demonstrated the dynamic changes in spinal cord compression, which was significantly increased during neck extension. In contrast, greater levels of compression may be placed on the spinal cord during neck flexion when the patients have OPLL with a high occupying rate.

➢ Key Points

- ❑ This study primarily evaluated dynamic factors in the pathogenesis of myelopathy in patients with cervical OPLL using kinematic CT myelography.
- ❑ This functional imaging study demonstrated that the spinal cord compression at the most compressed levels was significantly increased during neck extension compared with flexion.
- ❑ Spinal cord compression can increase during neck flexion when patients have OPLL with a high occupying rate.
- ❑ This study shows that dynamic factors play an important role in the development of myelopathy in patients with OPLL.

References

1. Clark CR. Cervical spondylotic myelopathy: History and physical findings. *Spine (Phila Pa 1976)* 1988;13:847–9.
2. Matsunaga S, Sakou T. Ossification of the posterior longitudinal ligament of the cervical spine: etiology and natural history. *Spine (Phila Pa 1976)* 2012;37:E309–14.
3. Inufusa A, An HS, Lim TH, et al. Anatomic changes of the spinal canal and intervertebral foramen associated with flexion-extension movement. *Spine (Phila Pa 1976)* 1996;21:2412–20.
4. Wang B, Liu H, Wang H, et al. Segmental instability in cervical spondylotic myelopathy with severe disc degeneration. *Spine (Phila Pa 1976)* 2006;31:1327–31.
5. Zhang L, Zeitoun D, Rangel A, et al. Preoperative evaluation of the cervical spondylotic myelopathy with flexion-extension magnetic resonance imaging: about a prospective study of fifty patients. *Spine (Phila Pa 1976)* 2011;36:E1134–9.
6. Azuma Y, Kato Y, Taguchi T. Etiology of cervical myelopathy induced by ossification of the posterior longitudinal ligament: determining the responsible level of OPLL myelopathy by correlating static compression and dynamic factors. *J Spinal Disord Tech* 2010;23:166–9.
7. Masaki Y, Yamazaki M, Okawa A, et al. An analysis of factors causing poor surgical outcome in patients with cervical myelopathy due to ossification of the posterior longitudinal ligament: anterior decompression with spinal fusion versus laminoplasty. *J Spinal Disord Tech* 2007;20:7–13.
8. Ogawa Y, Chiba K, Matsumoto M, et al. Long-term results after expansive open-door laminoplasty for the segmental-type of ossification of the posterior longitudinal ligament of the cervical spine: a comparison with nonsegmental-type lesions. *J Neurosurg Spine* 2005;3:198–204.
9. Yu YL, du Boulay GH, Stevens JM, et al. Computed tomography in cervical spondylotic myelopathy and radiculopathy: visualisation of structures, myelographic comparison, cord measurements and clinical utility. *Neuroradiology* 1986;28:221–36.
10. Batzdorf U, Flannigan BD. Surgical decompressive procedures for cervical spondylotic myelopathy. A study using magnetic resonance imaging. *Spine (Phila Pa 1976)* 1991;16:123–7.
11. Maus TP. Imaging of spinal stenosis: neurogenic intermittent claudication and cervical spondylotic myelopathy. *Radiol Clin North Am* 2012;50:651–79.
12. Chen CJ, Hsu HL, Niu CC, et al. Cervical degenerative disease at flexion-extension MR imaging: prediction criteria. *Radiology* 2003;227:136–42.
13. Miura J, Doita M, Miyata K, et al. Dynamic evaluation of the spinal cord in patients with cervical spondylotic myelopathy using a kinematic magnetic resonance imaging technique. *J Spinal Disord Tech* 2009;22:8–13.
14. Muhle C, Metzner J, Weinert D, et al. Classification system based on kinematic MR imaging in cervical spondylitic myelopathy. *AJNR Am J Neuroradiol* 1998;19:1763–71.
15. Machino M, Yukawa Y, Ito K, et al. Dynamic changes in dural sac and spinal cord cross-sectional area in patients with cervical spondylotic myelopathy: cervical spine. *Spine (Phila Pa 1976)* 2011;36:399–403.
16. Yamazaki T, Suzuki K, Yanaka K, et al. Dynamic computed tomography myelography for the investigation of cervical degenerative disease. *Neurol Med Chir (Tokyo)* 2006;46:210–5; discussion 215–6.

17. Wolfla CE, Snell BE, Honeycutt JH. Cervical ventral epidural pressure response to graded spinal canal compromise and spinal motion. *Spine (Phila Pa 1976)* 2004;29:1524–9.
18. Hirabayashi K, Miyakawa J, Satomi K, et al. Operative results and postoperative progression of ossification among patients with ossification of cervical posterior longitudinal ligament. *Spine (Phila Pa 1976)* 1981;6:354–64.
19. Hori T, Kawaguchi Y, Kimura T. How does the ossification area of the posterior longitudinal ligament thicken following cervical laminoplasty? *Spine (Phila Pa 1976)* 2007;32:E551–6.
20. Kawaguchi Y, Urushisaki A, Seki S, et al. Evaluation of ossification of the posterior longitudinal ligament by three-dimensional computed tomography and magnetic resonance imaging. *Spine J* 2011;11:927–32.
21. Sakai K, Okawa A, Takahashi M, et al. Five-year follow-up evaluation of surgical treatment for cervical myelopathy caused by ossification of the posterior longitudinal ligament: a prospective comparative study of anterior decompression and fusion with floating method versus laminoplasty. *Spine (Phila Pa 1976)* 2012;37:367–76.
22. Iwasaki M, Okuda S, Miyauchi A, et al. Surgical strategy for cervical myelopathy due to ossification of the posterior longitudinal ligament: Part 1: Clinical results and limitations of laminoplasty. *Spine (Phila Pa 1976)* 2007;32:647–53.
23. Iwasaki M, Okuda S, Miyauchi A, et al. Surgical strategy for cervical myelopathy due to ossification of the posterior longitudinal ligament: Part 2: Advantages of anterior decompression and fusion over laminoplasty. *Spine (Phila Pa 1976)* 2007;32:654–60.
24. Matsunaga S, Kukita M, Hayashi K, et al. Pathogenesis of myelopathy in patients with ossification of the posterior longitudinal ligament. *J Neurosurg* 2002;96(2 suppl):168–72.
25. Tani T, Ushida T, Ishida K, et al. Relative safety of anterior microsurgical decompression versus laminoplasty for cervical myelopathy with a massive ossified posterior longitudinal ligament. *Spine (Phila Pa 1976)* 2002;27:2491–8.
26. Fujiyoshi T, Yamazaki M, Okawa A, et al. Static versus dynamic factors for the development of myelopathy in patients with cervical ossification of the posterior longitudinal ligament. *J Clin Neurosci* 2010;17:320–4.
27. Mochizuki M, Aiba A, Hashimoto M, et al. Cervical myelopathy in patients with ossification of the posterior longitudinal ligament. *J Neurosurg Spine* 2009;10:122–8.
28. Chang H, Song KJ, Kim HY, et al. Factors related to the development of myelopathy in patients with cervical ossification of the posterior longitudinal ligament. *J Bone Joint Surg Br* 2012;94:946–9.
29. Ogawa Y, Toyama Y, Chiba K, et al. Long-term results of expansive open-door laminoplasty for ossification of the posterior longitudinal ligament of the cervical spine. *J Neurosurg Spine* 2004;1:168–74.
30. Matsumoto M, Chiba K, Toyama Y. Surgical treatment of ossification of the posterior longitudinal ligament and its outcomes: posterior surgery by laminoplasty. *Spine (Phila Pa 1976)* 2012;37:E303–8.
31. Seichi A, Hoshino Y, Kimura A, et al. Neurological complications of cervical laminoplasty for patients with ossification of the posterior longitudinal ligament-a multi-institutional retrospective study. *Spine (Phila Pa 1976)* 2011;36:E998–1003.
32. Matsuoka T, Yamaura I, Kurosa Y, et al. Long-term results of the anterior floating method for cervical myelopathy caused by ossification of the posterior longitudinal ligament. *Spine (Phila Pa 1976)* 2001;26:241–8.

Spine

SPINE Volume 39, Number 3, pp E159-E165

CERVICAL SPINE

Efficacy of Biphasic Transcranial Electric Stimulation in Intraoperative Motor Evoked Potential Monitoring for Cervical Compression Myelopathy

Dai Ukegawa, MD, Shigenori Kawabata, MD, PhD, Kyohei Sakaki, MD, PhD, Senichi Ishii, MD, PhD, Shoji Tomizawa, MD, PhD, Hiroyuki Inose, MD, PhD, Toshitaka Yoshii, MD, PhD, Tsuyoshi Kato, MD, PhD, Mitsuhiro Enomoto, MD, PhD, and Atsushi Okawa, MD, PhD

Study Design. Retrospective analysis of prospectively collected data from consecutive patients undergoing 2 methods of transcranial electrical motor evoked potential (TCE-MEP) monitoring during cervical spine surgery.

Objective. To investigate the efficacy of biphasic transcranial electric stimulation, the deviation rate, amplitude of TCE-MEPs, complications, and sensitivity and specificity of TCE-MEP monitoring were compared between the biphasic and conventional monophasic stimulation methods.

Summary of Background Data. With biphasic stimulation, unlike monophasic stimulation, measurement time can be reduced considerably because a single stimulation elicits bilateral responses almost simultaneously. However, no study has yet reported a detailed comparison of the 2 methods.

Methods. *Examination 1:* Amplitude and derivation rate of TCE-MEPs was compared for monophasic and biphasic stimulation in the same 31 patients with cervical compression myelopathy. *Examination 2:* Sensitivity, specificity, and complications of TCE-MEP monitoring were compared in 200 patients with cervical compression myelopathy who received monophasic or biphasic stimulation (100 patients each) during intraoperative monitoring.

Results. *Examination 1:* Derivation rates of biphasic stimulation in the deltoid, biceps brachii, abductor digiti minimi, and flexor hallucis brevis muscles were the same or higher than for monophasic stimulation. TCE-MEP amplitudes elicited by biphasic stimulation compared with monophasic stimulation were significantly larger in the biceps (paired t, $P < 0.0001$), but similar in the other 3 muscles. *Examination 2:* In the biphasic and monophasic stimulation groups, warnings were issued to surgeons in 10 and 11 cases, for a sensitivity of 100% for both groups and specificity of 97.8% and 96.7%, respectively. No complications related to stimulation were observed in any of the 200 patients.

Conclusion. Biphasic stimulation had similar or higher derivation rates and equivalent sensitivity and specificity than monophasic stimulation. No complications were observed for either stimulation method. Biphasic stimulation is an effective TCE-MEP monitoring method for cervical spine surgery that may also reduce measurement time.

Key words: biphasic transcranial electric stimulation, intraoperative monitoring of spinal cord, patients with cervical compression myelopathy, sensitivity, specificity.

Level of Evidence: 4

Spine 2014;39:E159–E165

Intraoperative spinal cord monitoring is attracting attention because of its key role in preventing neurological impairment during spinal cord surgery.[1,2] Monitoring of transcranial electrical motor evoked potentials (TCE-MEP, compound muscle action potentials) is one of the most widely used intraoperative monitoring techniques today, and by measuring multiple electromyograms it can monitor each bilateral and segmental function of gray as well as white matter. TCE-MEP monitoring offers many advantages including noninvasive monitoring of motor systems.[3–8] Transcranial stimulation predominantly stimulates the brain on the anode side, evoking large muscle evoked potentials on the contralateral side.[9,10] Consequently, in conventional monophasic stimulation,[11] it is necessary to switch the polarity of stimulation (from right anode–left cathode to right cathode–left anode)[12] to study muscle responses on both sides.[13,14] In biphasic stimulation, on the contrary, a second reversed-phase stimulation follows immediately after the first stimulation, thus stimulating both sides of the brain almost simultaneously. Consequently, this

Department of Orthopaedic Surgery, Tokyo Medical and Dental University, Yushima, Bunkyo-ku, Tokyo, Japan.

Acknowledgment date: October 15, 2012. First revision date: July 29, 2013. Acceptance date: October 12, 2013.

The device(s)/drug(s) is/are FDA-approved or approved by corresponding national agency for this indication.

The Ministry of Health, Labour and Welfare of Japan research grant funds were received, in part, to support this work.

Relevant financial activities outside the submitted work: payment for writing or reviewing the manuscript and grants/grants pending.

Address correspondence and reprint requests to Shigenori Kawabata, MD, PHD, Department of Orthopaedic Surgery, Tokyo Medical and Dental University, 1-5-45 Yushima, Bunkyo-ku, Tokyo 113-8510, Japan; E-mail: kawabata.orth@tmd.ac.jp

DOI: 10.1097/BRS.0000000000000082

method enables the evaluation of spinal cord functions on both sides using a train of biphasic stimulus pulses without the need to reverse the polarity. This is likely to reduce intraoperative measurement time and thus interruption time. However, no previous TCE-MEP study has compared biphasic and conventional monophasic stimulation in detail.

In examination 1 of this study, to elucidate the efficacy of biphasic stimulation, we performed both biphasic and monophasic stimulation in patients with cervical compression myelopathy and compared the derivation rate and amplitude of TCE-MEP responses obtained by the 2 methods. In examination 2, we performed either method for intraoperative monitoring in 200 patients with cervical compression myelopathy (100 patients for each method) to assess the accuracy of the monitoring system and examine complications.

MATERIALS AND METHODS

Examination 1

We recruited 31 patients with cervical compression myelopathy who had received TCE-MEP intraoperative monitoring at our hospital between September 2010 and June 2011. Patients requiring reoperation were excluded. Neuromaster MEE-1200 and MS-120B (Nihon Kohden, Tokyo, Japan) systems were used for the measurement and analysis of evoked potentials. This study was approved by the Ethics Committee of the School of Medicine, Tokyo Medical and Dental University, and was performed with written informed consent from patients and followed all the guidelines for experimental investigation with human subjects required by the institutional guidelines.

All patients received general anesthesia through continuous intravenous injection of propofol (4.5 mg/kg/hr), and the injected dose was adjusted to maintain the bispectral index on the bispectral monitor in a range of 40 to 60. The muscle relaxant rocuronium bromide was administered at the minimum amount (17.1 ± 21.3 mg [mean ± standard deviation], range 0–50 mg). The analgesic remifentanil (0.25–0.5 μg/kg/min) was administered continuously. L-shaped stimulation electrodes for transcranial stimulation were inserted into the scalp to rest on the skull. Stimulation sites were symmetrical, at 2-cm anterior and 5-cm symmetric to Cz (international 10–20 system). Approximately, 30 minutes after the induction of anesthesia when the effect of the muscle relaxant had reduced and the depth of anesthesia stabilized, the 2 methods of stimulation were performed and TCE-MEPs were measured.

For monophasic stimulation, through the right anode and left cathode stimulation electrodes, a train of 5 monophasic rectangular pulses, 200-mA intensity and 0.5-millisecond duration, were applied at a frequency of 1 Hz with interstimulus intervals of 2 milliseconds. After 5 to 10 pulses,

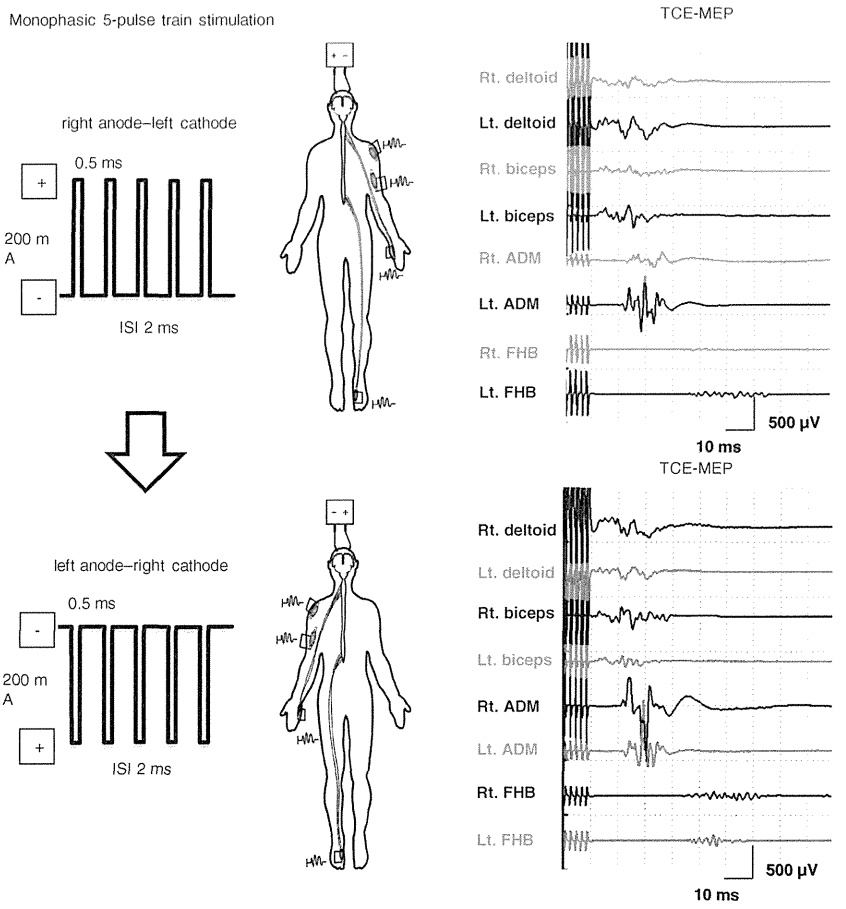

Figure 1. Stimulus condition, recorded muscles, and TCE-MEPs for monophasic stimulation. Polarity must be switched to study muscle responses on both sides. TCE-MEP indicates transcranial electrical motor evoked potential; FHB, flexor hallucis brevis; ADM, abductor digiti minimi; rt., right; lt., left.

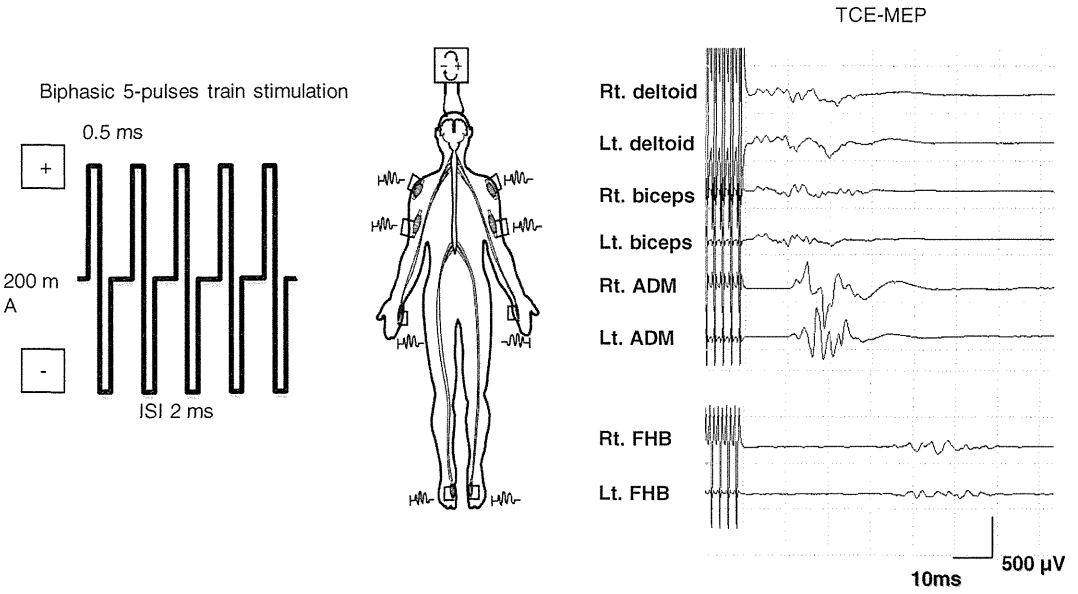

Figure 2. Stimulus condition, recorded muscles, and TCE-MEPs for biphasic stimulation. TCE-MEPs are elicited almost simultaneously on both sides. TCE-MEP indicates transcranial electrical motor evoked potential; FHB, flexor hallucis brevis; ADM, abductor digiti minimi; rt., right; lt., left.

mean values were obtained. After polarity was reversed, TCE-MEP was measured under the same conditions (Figure 1). For biphasic stimulation, a 200-mA and 0.5-millisecond rectangular pulse, as in monophasic stimulation, was immediately followed by an opposite rectangular pulse to produce 1 biphasic pulse. A train of 5 pulses were applied at a frequency of 1 Hz with an interstimulus interval of 2 milliseconds, and after 5 to 10 pulses, mean values were obtained (Figure 2). In both methods, TCE-MEPs were recorded bilaterally from the deltoid (Del), biceps brachii (Bic), abductor digiti minimi (ADM), and flexor hallucis brevis (FHB) muscles. For monophasic stimulation, the TCE-MEP study was conducted using the left muscle responses by right anode stimulation and the right muscle responses by left anode stimulation. Data were analyzed using GraphPad Prism5 statistical software (GraphPad Software, Inc., San Diego, CA).

Parameters assessed were age, sex, type of disorder, and upper and lower extremity motor function scores obtained preoperatively in accordance with the Japanese Orthopedic Association Score System for Cervical Myelopathy (upper and lower extremity JOAs) (see Supplemental Digital Content 1, Table 1 available at http://links.lww.com/BRS/A851).[15] Intraoperative derivation rates and peak-to-peak amplitudes of Del, Bic, ADM, and FHB were compared between the 2 methods. Because a certain amplitude level is needed in TCE-MEP monitoring for successful evaluation of spinal cord motor function, amplitudes that were not stably 5 μV or more were regarded as "no derivation."

Examination 2

We recruited 200 patients with cervical compression myelopathy who had received either monophasic (100 patients) or biphasic (100 patients) stimulation between May 2007 and April 2010 or August 2009 and June 2012, respectively, at our hospital. Patients requiring reoperation were excluded. Electromyograms were recorded using Neuropack (MEB-2200) or Neuromaster (MEE-1200) from Nihon Kohden Co. Method of anesthesia, TCE stimulation, and MEP recording were the same as those in Examination 1. Moreover, in all cases TCE-MEP was combined with transcranial electrical simulated spinal cord evoked potential (TCE-SCEP) monitoring (single rectangular pulse, 200-mA intensity, 0.5-millisecond duration, and 3-Hz frequency). TCE-SCEP was recorded by bipolar derivation from epidural electrodes (Unique Medical, Tokyo, Japan) placed before surgery, using a Tuohy needle in the lower thoracic epidural space (Th11–T12). The distance between the electrodes was 15 mm. Consecutive potentials (20–50) were averaged and recorded.

Because our hospital had previously experienced cases of tooth damage or tongue injury during transcranial stimulation, wads of gauze rolled into a cylindrical shape were used as a bite block in all cases. In the monophasic stimulation group, the operating surgeon was warned only when the TCE-MEP wave disappeared concomitant with an amplitude decrease of 50% or more on TCE-SCEP. For the biphasic stimulation group, we adopted warning thresholds reported by Sakaki *et al.*[16] We defined TCE-MEPs recorded from the muscles innervated by the spinal levels exposed to surgical invasion (*e.g.*, upper limb muscles in cervical spine surgery) as segmental potentials. Similarly, TCE-MEPs recorded from the muscles innervated distal to the levels of the spinal cord exposed to decompression (*e.g.*, lower limb muscles in cervical spine surgery) were used as spinal tract potentials. Surgeons were warned when the TCE-MEP amplitude for the spinal segments became 30% of the control amplitude or when the TCE-MEP amplitude for the spinal tract disappeared concomitant with a

TCE-SCEP amplitude decrease of 50% or more. At the time of warning, if a certain surgical maneuver or potential causal factor of neurological impairment was identified, surgery was discontinued until the amplitude recovered or the causal factor was removed. The number of warnings, cases of postoperative neuronal impairment, and monitoring-related complications were compared between the 2 groups.

Moreover, to estimate the sensitivity and specificity of TCE-MEP monitoring properly after each stimulation methods, intraoperative amplitude change on TCE-MEP without using TCE-SCEP were re-evaluated retrospectively in both stimulation groups, adopting the same warning thresholds.[16]

This study was approved by the Ethics Committee of the School of Medicine, Tokyo Medical and Dental University, and was performed with written informed consent and followed all the guidelines for experimental investigation with human subjects required by the institutional guidelines.

RESULTS

Examination 1

Among the 31 cases, 20 involved cervical spondylotic myelopathy, 1 cervical disc herniation, 4 ossification of the posterior longitudinal ligament of the cervical spine, 4 cervical spinal cord tumor (all extramedullary tumor), 1 cervical spondylotic amyotrophy, and 1 ossification ligamentum flavum of the cervical spine. Patients were 22 males and 9 females aged 63.1 ± 16.0 (26–89) years with upper and lower extremity JOA motor function scores of 1.87 ± 1.30 (−1–4) and 1.87 ± 1.14 (0–4) points, respectively.

Among a total of 62 muscles on both sides tested, potentials were not evoked by monophasic stimulation in 3 Del (derivation rate 95.2%), 2 Bic (96.8%), 4 ADM (93.5%), and 6 FHB (90.3%) muscles or by biphasic stimulation in 3 Del (95.2%), 2 Bic (96.8%), 2 ADM (96.8%), and 4 FHB (93.5%) muscles. When the relation between JOA motor function score of the upper extremity and TCE-MEPs of the upper extremity muscles (Del, Bic, and ADM) were analyzed, both types of stimulation evoked potentials in all muscles on both sides in all patients with an upper extremity JOA motor function score of 4–3 but not in those with a score of zero.

With regard to the relation between lower extremity JOA motor function score and FHB potentials, monophasic stimulation evoked potentials in all muscles on both sides in all patients with a lower extremity JOA motor function score of 4–3 and biphasic stimulation evoked potentials in those with a score of 4–2. In both methods, the derivation rate was 50% in patients with a score of 0.

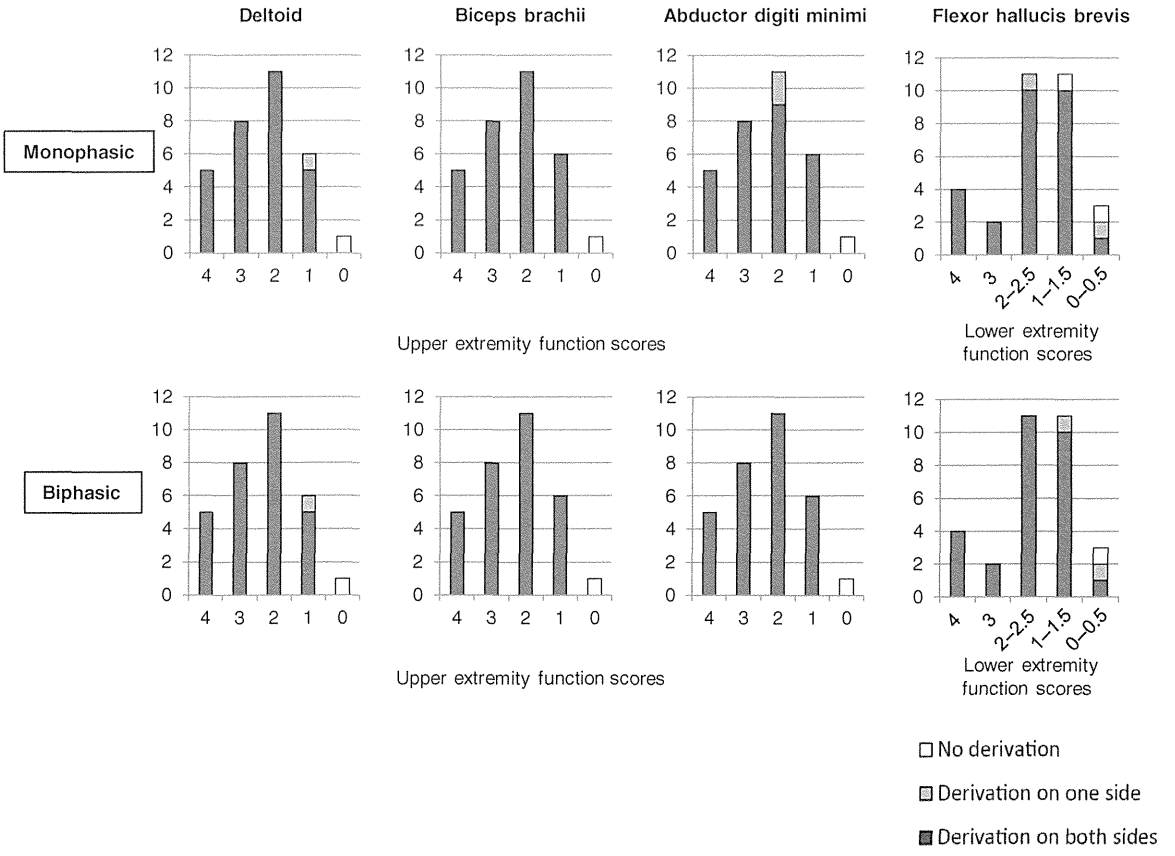

Figure 3. Relation between JOA upper extremity motor function score and upper extremity TCE-MEPs, and lower extremity JOA motor function score and FHB TCE-MEPs. TCE-MEP indicates transcranial electrical motor evoked potential; JOA, Japanese Orthopedic Association; FHB, flexor hallucis brevis.

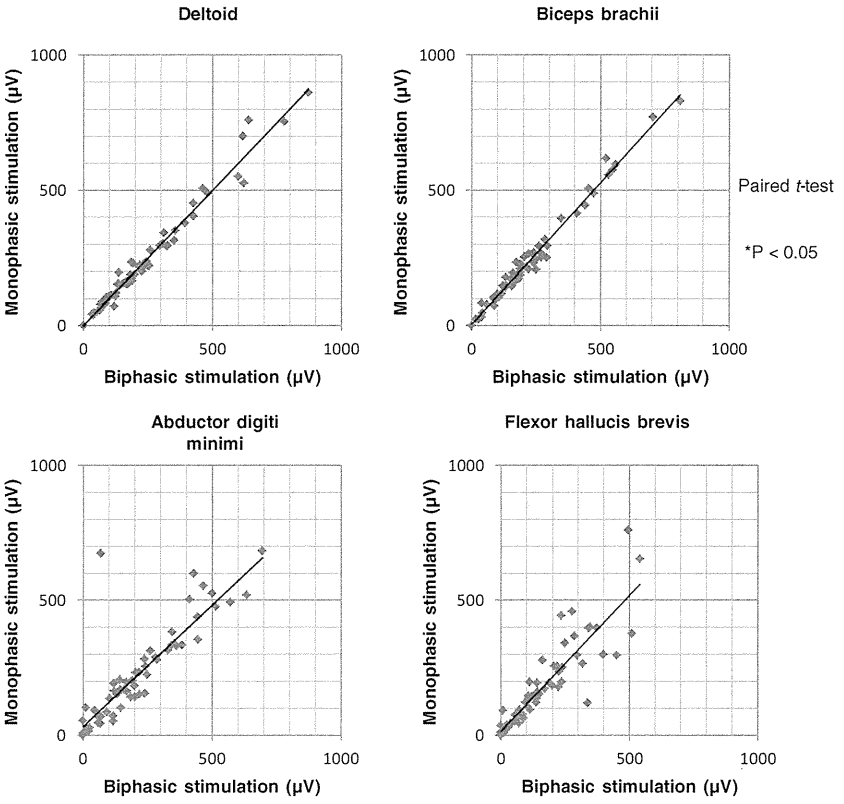

Figure 4. TCE-MEP amplitude of the same muscles was compared between the 2 stimulation methods in each patient. TCE-MEP indicates transcranial electrical motor evoked potential.

Del and Bic responded similarly to both stimulation methods. In 2 patients with a JOA motor function score of 2, ADM was evoked unilaterally by monophasic stimulation but bilaterally by biphasic stimulation. For FHB, cases in which monophasic stimulation evoked potentials either unilaterally or on neither side were evoked by biphasic stimulation either bilaterally or unilaterally. When biphasic stimulation did not evoke potentials in any muscles, these muscles also showed no potentials under monophasic stimulation (Figure 3).

TCE-MEP amplitude of the same muscles was compared between the 2 stimulation methods in each patient. The amplitude of the dominant muscles under monophasic stimulation (left or right muscles stimulated through the right or left anode, respectively) was similar to that under biphasic stimulation, except that the TCE-MEP amplitude of Bic was significantly larger under the latter method (paired t test, $P < 0.0001$, Figure 4).

Examination 2

In the biphasic stimulation group, data were collected from 100 patients (71 males, 29 females) aged 64.5 ± 12.7 (26–89) years with upper and lower extremity JOA motor function scores of 2.00 ± 1.21 (−1–4) and 1.94 ± 1.19 (0–4) points, respectively. There were 60 cases of cervical spondylotic myelopathy, 4 of cervical disc herniation, 23 of ossification of the posterior longitudinal ligament of the cervical spine, 8 of extramedullary spinal cord tumor, 2 of cervical spondylotic amyotrophy, 1 of ossification ligamentum flavum, and 2 of rheumatoid spondylitis. In the monophasic stimulation group, 100 patients (77 males, 23 females) aged 63.0 ± 12.6 (35 to 89) years with upper and lower extremity JOA motor function scores of 2.16 ± 1.13 (−2–4) and 2.00 ± 1.20 (0–4) points, respectively, were categorized into 60 cases of cervical spondylotic myelopathy, 10 of cervical disc herniation, 25 of ossification of the posterior longitudinal ligament of the cervical spine, 2 of extramedullary spinal cord tumors, 1 of atlantoaxial subluxation, and 2 of upper cervical pseudotumor. There were no significant differences in type of disorder, sex, age, or upper or lower extremity JOA motor function scores between the groups.

Under biphasic stimulation, we could not obtain valid TCE-MEPs for intraoperative monitoring in 1 case, and we gave an actual warning to the surgeon in 9 cases, in 7 of which the surgeon discontinued surgery temporarily or removed the causal factor in response. Waveforms were recovered in only 4 cases, but none of the 7 developed postoperative paralysis. The remaining 2 cases, in which the surgeon did not respond, did not recover the waveforms and segmental motor paralysis developed in 1 of the cases (*i.e.*, the Schwannoma case). No postoperative paralysis was observed in the 90 cases requiring no intraoperative warning. If we had disregarded TCE-SCEP and applied the warning threshold[16] to TCE-MEP monitoring, warnings would have been given in 10 cases and not in 89 cases. No postoperative paralysis developed in 7 of the 10 cases when the surgeon responded promptly. However, in 1 of the remaining 3 cases in which the surgeon did not respond, postoperative paralysis occurred. With the exclusion of 1 case without valid TCE-MEPs and 7 cases of prompt response, the sensitivity and

specificity of TCE-MEP monitoring using the biphasic method would have been 100% and 97.8%, respectively.

Under monophasic stimulation, we could not obtain valid TCE-MEPs in 1 case and we gave actual warnings in 4 cases. The surgeon responded in all cases, but waveforms resumed in only 1 case; in the other 3 cases, 1 (*i.e.*, the meningioma case) developed postoperative segmental motor paralysis. No postoperative paralysis was observed in 95 cases requiring no intraoperative warning. If we had disregarded TCE-SCEP and applied the warning thresholds[16] to TCE-MEP monitoring, warnings would have been given in 11 cases and not in 88 cases. Of these 11 cases, the surgeon responded in 4, 1 of which developed postoperative paralysis. Of the 7 cases in which the surgeon did not respond, waveforms recovered in only 4 cases, but none of the 7 developed postoperative paralysis. In addition, no paralysis was observed in cases requiring no warning. With the exclusion of the 1 case without valid TCE-MEPs, 4 cases with a prompt response, and 4 cases with spontaneous waveform recovery despite the surgeon's lack of response, the sensitivity and specificity of TCE-MEP monitoring using the monophasic method would have been 100% and 96.7%, respectively.

There were no signs of complications such as burns, tooth damage, alveolar ridge injury, or seizures in either group.

DISCUSSION

In examination 1, although TCE-MEPs in patients with severe paralysis were difficult to evoke by biphasic or monophasic stimulation, the derivation rates were generally the same or higher under biphasic stimulation than under monophasic stimulation. This might have been due to the firing of pyramidal neurons in the brain by the opposite rectangular pulse despite the absence of firing evoked by the initial 200-mA monophasic stimulation. Alternatively, it might have been caused by anterior horn cells in the spinal cord segments firing due to activation of the contralateral descending pathway by the opposite rectangular pulse despite the absence of firing evoked by the initial monophasic stimulation. In addition, similar TCE-MEP amplitudes were obtained by both methods, although biphasic stimulation evoked significantly greater Bic amplitudes than monophasic stimulation. It is also possible that the significant difference in Bic amplitudes was caused by the large derivation rate and stable amplitude of Bic potentials despite unstable amplitudes in Del due to stimulation artifacts and in ADM and FHB due to spinal cord impairment. We plan to increase the number of cases to perform more detailed studies. However, thus far, the findings suggest that biphasic stimulation results in similar or superior potentials in the target muscles compared with monophasic stimulation for which the polarity needs to be reversed to obtain TCE-MEP from both sides.

The warning criteria used under monophasic stimulation are controversial. Hsu *et al*[17] set the warning threshold during spinal cord surgery to 50% or more of the amplitude lasting for at least 1 minute, and achieved a sensitivity of 100% and specificity of 97% in 172 patients.[17] In another study of 52 patients with cervical compression myelopathy, Kim *et al*[18] set the warning threshold at an amplitude decrease of 80% or more and reported 100% sensitivity and 90% specificity. Furthermore, Sakaki *et al*[16] operated on 350 patients with cervical compression myelopathy using different warning thresholds based on the spinal tracts and segments (30% of control segmental potentials and disappearance of the tract potentials) and found a sensitivity and specificity of 100% and 83.7%, respectively.

We used different warning criteria in the monophasic and biphasic groups at our institution. Warning criteria need to be as similar as possible to compare the sensitivity and specificity of the 2 stimulation methods properly. We therefore established hypothetical warning criteria in examination 2 to analyze the changes in TCE-MEP waveforms retrospectively. We disregarded changes in TCE-SCEP waveforms in both groups and determined the sensitivity and specificity based on the presence/absence of postoperative paralysis with the assumptions that warnings were given because of TCE-MEP amplitudes for segmental potentials had decreased to less than 30% of the control value and waveforms of spinal tract potentials had disappeared. Because this was a retrospective analysis, we excluded cases in which the surgeon responded promptly and in which the TCE-MEP waveforms recovered after decreasing or disappearing temporarily. Although this may not be the most appropriate way to compare 2 stimulation methods, we think the present findings are valuable because this study was conducted at a single institution by the same research group. The analysis showed that sensitivity and specificity would have been 100% and 96.7% under monophasic stimulation and 100% and 97.8% under biphasic stimulation, respectively. Thus, both methods were shown to be equally effective.

To elucidate TCE-MEP–related complications, MacDonald[19] investigated 15,000 cases reported in various studies and found 5 cases of seizures, 29 of injury to the teeth and gums, 1 of mandibular fracture, 5 of arrhythmia, 1 of intraoperative awakening, and 1 of burn injury at the site of stimulation. Schwartz *et al*[20] observed 26 cases (0.14%) of TCE-MEP–related complications in 18,862 patients. In examination 2 of this study in which 100 patients were stimulated using one of the methods, there were no such complications. Although the number of patients may not be large, this study demonstrates that the safety of stimulation is similar for both methods.

CONCLUSION

Compared with monophasic stimulation, single biphasic TCE stimulation can elicit MEPs on both sides during intraoperative neurophysiological monitoring, reducing measurement time by half. This also reduces the time surgeons spend standing by as well as overall operation time. Our findings clearly show that, compared with monophasic stimulation, biphasic stimulation produces similar sensitivity, specificity, safety, the same or higher derivation rates, and similar or superior potentials and convenience, and thus promises to be an effective method of transcranial stimulation.

➢ Key Points

- ❑ Both biphasic and monophasic stimulation were performed in 31 patients with cervical compression myelopathy to compare the transcranial electrical motor evoked potentials (TCE-MEPs) of recorded muscles. Deviation rates and amplitudes elicited by biphasic stimulation were either the same or higher than those obtained by monophasic stimulation.
- ❑ TCE-MEP monitoring in 100 patients with cervical compression myelopathy undergoing biphasic stimulation had similar sensitivity and specificity compared with another 100 patients with cervical compression myelopathy undergoing monophasic stimulation. None of the patients in either group experienced complications related to stimulation.
- ❑ Biphasic stimulation was comparable with monophasic stimulation in terms of deviation rate, sensitivity, specificity, and safety, suggesting that it is an effective method for TCE-MEP monitoring during cervical spine surgery.

Supplemental digital content is available for this article. Direct URL citation appearing in the printed text is provided in the HTML and PDF version of this article on the journal's web site (www.spinejournal.com).

References

1. DeVrin VJ, Schwartz DM. Intraoperative neurophysiologic monitoring during spinal surgery. *J Am Acad Orthop Surg* 2007;15:549–60.
2. Tamaki T, Kubota S. History of the development of intraoperative spinal cord monitoring. *Eur Spine J* 2007;16(suppl 2):140–6.
3. Levy WJ. Motor evoked potentials from transcranial stimulation of the motor cortex in human. *Neurosurg* 1984;15:287–302.
4. Barker AT. Non-invasive magnetic stimulation of human motor cortex. *Lancet* 1985;1:1106–7.
5. Kitagawa H, Itoh T, Takano H, et al. Motor evoked potential monitoring during upper cervical spine surgery. *Spine* 1989;14:1078–83.
6. Sala F, Palandri G, Basso E, et al. Motor evoked potential monitoring improves outcome during spine surgery for intramedullary spinal cord tumor. *Neurosurgery* 2006;58:1129–43.
7. Fulkerson DH, Satyan KB, Wilder LM, et al. Intraoperative monitoring of motor evoked potentials in very young children. *J Neurosurg Pediatr* 2011;7:331–7.
8. Møller AR, Ansari S, Cohen-Gadol AA, et al. Techniques of intraoperative monitoring for spinal cord function: their past, present, and future directions. *Neurol Res* 2011;33:363–70.
9. Jones SJ, Harrison R, Koh KF, et al. Motor evoked potential monitoring during spinal surgery: responses of distal limb muscles to transcranial cortical stimulation with pulse trains. *Electroencephalogr Clin Neurophysiol* 1996;100:375–83.
10. Pechstein U, Cedzich C, Nadstawek J, et al. Transcranial high-frequency repetitive electrical stimulation for recording myogenic motor evoked potentials with the patient under general anesthesia. *Neurosurgery* 1996;39:335–44.
11. Mochida K, Shinomiya K, Komori H, et al. A new method of multisegment motor pathway monitoring using muscle potentials after train spinal stimulation. *Spine* 1995;20:2240–6.
12. MacDonald DB. Intraoperative motor evoked potential monitoring: overview and update. *J Clin Monit Comput* 2006;20:347–77.
13. Deletis V, Sala F. Intraoperative neurophysiological monitoring of the spinal cord during spinal cord and spine surgery: a review focus on the corticospinal tracts. *Clin Neurophysiol* 2008;119:248–64.
14. Kempton LB, Nantau WE, Zaltz I. Successful monitoring of transcranial electrical motor evoked potentials with isoflurane and nitrous oxide in scoliosis surgeries. *Spine* 2009;35:1627–9.
15. Hirabayashi K, Miyakawa J, Satomi K, et al. Operative results and postoperative progression of ossification among patients with ossification of cervical posterior longitudinal ligament. *Spine (Phila Pa 1976)* 1981;6:354–64.
16. Sakaki K, Kawabata S, Ukegawa D, et al. Warning thresholds on the basis of origin of amplitude changes in transcranial electrical motor evoked potential monitoring for cervical compression myelopathy. *Spine* 2012;37:913–21.
17. Hsu B, Cree AK, Lagopoulos J, et al. Transcranial motor-evoked potentials combined with response recording through compound muscle action potential as the sole modality of spinal cord monitoring in spinal deformity surgery. *Spine* 2008;33:1100–06.
18. Kim DH, Zaremski J, Kwon B, et al. Risk factors for false positive transcranial motor evoked potential monitoring alerts during surgical treatment of cervical myelopathy. *Spine* 2007;32:3041–6.
19. MacDonald DB. Safety of intraoperative transcranial electrical stimulation motor evoked potential monitoring. *J Clin Neurophysiol* 2002;19:416–29.
20. Schwartz DM, Sestokas AK, Dormans JP, et al. Transcranial electric motor evoked potential monitoring during spine surgery: is it safe? *Spine* 2011;36:1046–9.

Stem Cell Reports
Report
OPEN ACCESS

Stepwise Differentiation of Pluripotent Stem Cells into Osteoblasts Using Four Small Molecules under Serum-free and Feeder-free Conditions

Kosuke Kanke,[1,2] Hideki Masaki,[6,7] Taku Saito,[2,4] Yuske Komiyama,[5] Hironori Hojo,[1] Hiromitsu Nakauchi,[6,7] Alexander C. Lichtler,[8] Tsuyoshi Takato,[2] Ung-il Chung,[1,3] and Shinsuke Ohba[1,3,*]
[1]Center for Disease Biology and Integrative Medicine
[2]Department of Sensory and Motor System Medicine
[3]Department of Bioengineering
[4]Department of Bone and Cartilage Regenerative Medicine
[5]Intensive Care Unit
The University of Tokyo, Tokyo 113-0033, Japan
[6]Japan Science Technology Agency, ERATO, Nakauchi Stem Cell and Organ Regeneration Project
[7]Division of Stem Cell Therapy, Center for Stem Cell Biology and Regenerative Medicine, Institute of Medical Science
The University of Tokyo, Tokyo 108-8639, Japan
[8]Department of Reconstructive Sciences, School of Dental Medicine, University of Connecticut Health Center, Farmington, CT 06030, USA
*Correspondence: ohba@bioeng.t.u-tokyo.ac.jp
http://dx.doi.org/10.1016/j.stemcr.2014.04.016

SUMMARY

Pluripotent stem cells are a promising tool for mechanistic studies of tissue development, drug screening, and cell-based therapies. Here, we report an effective and mass-producing strategy for the stepwise differentiation of mouse embryonic stem cells (mESCs) and mouse and human induced pluripotent stem cells (miPSCs and hiPSCs, respectively) into osteoblasts using four small molecules (CHIR99021 [CHIR], cyclopamine [Cyc], smoothened agonist [SAG], and a helioxanthin-derivative 4-(4-methoxyphenyl)pyrido[4′,3′:4,5]thieno [2,3-b]pyridine-2-carboxamide [TH]) under serum-free and feeder-free conditions. The strategy, which consists of mesoderm induction, osteoblast induction, and osteoblast maturation phases, significantly induced expressions of osteoblast-related genes and proteins in mESCs, miPSCs, and hiPSCs. In addition, when mESCs defective in runt-related transcription factor 2 (*Runx2*), a master regulator of osteogenesis, were cultured by the strategy, they molecularly recapitulated osteoblast phenotypes of *Runx2* null mice. The present strategy will be a platform for biological and pathological studies of osteoblast development, screening of bone-augmentation drugs, and skeletal regeneration.

INTRODUCTION

The limited number of osteoblasts that can be obtained from animals hinders the performance of extensive studies on protein interactions, transcriptional networks, and epigenetics in osteoblast development. Therefore, pluripotent stem cell-based osteogenic differentiation may be an attractive model for such studies, given the pluripotency and capacity for self-renewal of stem cells. Although several strategies have been used to differentiate pluripotent stem cells, including embryonic stem cells (ESCs) and induced pluripotent stem cells (iPSCs) into osteoblasts (Bilousova et al., 2011; Buttery et al., 2001; Li et al., 2010; Kao et al., 2010; Kawaguchi et al., 2005; Phillips et al., 2001; Tai et al., 2004; Ye et al., 2011; zur Nieden et al., 2003), none of these is a stepwise differentiation strategy that uses small molecule inducers and serum-free monolayer cultures without the formation of embryoid bodies (EBs).

Using the combination of a mitogen-activated protein kinase kinase (MEK) inhibitor, PD0325901 (PD03), and a glycogen synthase kinase 3 (GSK3) inhibitor, CHIR99021 (CHIR), which will hereafter be referred to as 2i, mouse ESCs (mESCs) are maintained in a ground state (Ying et al., 2008). CHIR activates canonical Wnt signaling by suppressing the degradation of β-catenin (Bain et al., 2007). Canonical Wnt signaling cues also specify the differentiation of germ layers and multipotent stem cells into mesodermal cells (Davis and Zur Nieden, 2008). We recently described the gene regulatory networks underlying canonical Wnt signaling-mediated control of mesoderm differentiation and pluripotency in mESCs (Zhang et al., 2013).

The formation of osteoblasts is a sequential process. In mesoderm-derived skeletons, cells in the lateral plate mesoderm or the paraxial mesoderm give rise to skeletal progenitors, which then differentiate into bone-forming osteoblasts and cartilage-forming chondrocytes (Akiyama et al., 2005). We and others have shown that hedgehog (Hh) signaling is essential for normal osteoblast development, particularly for the specification of osteo-chondroprogenitors into osteoblast precursors, which express runt-related transcription factor 2 (*Runx2*), a transcription factor essential for bone formation (Hojo et al., 2012; Long et al., 2004; St-Jacques et al., 1999); the smoothened (SMO) agonist (SAG), a Hh signaling activator, promoted early osteoblast differentiation in perichondrial cells, which consist of osteo-chondroprogenitors (Hojo et al., 2012). This finding suggested that SAG could efficiently

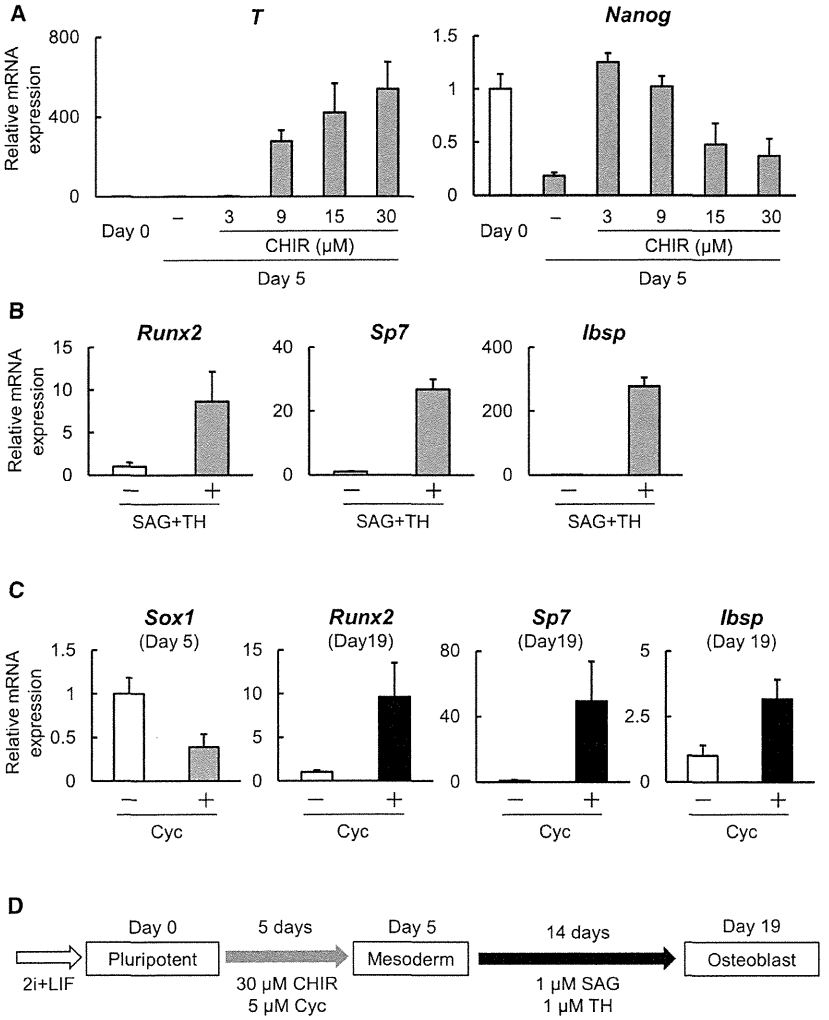

Figure 1. Optimization of Mesoderm Induction and Osteoblast Induction in mESCs

(A) The effect of the 5-day treatment with CHIR on mesoderm differentiation and the suppression of the pluripotent state in mESCs. 2i-cultured mESCs were treated for 5 days with CHIR at different concentrations. The mRNA expression levels were determined using RT-quantitative PCR (RT-qPCR). The data are expressed as the mean ± SEM from three independent experiments. See also Figure S1.

(B) The effect of the 14-day treatment with SAG plus TH on osteoblast differentiation of mESC-derived mesodermal cells. The mESCs were cultured with 30 μM CHIR for 5 days, then with (gray bars) or without (white bars) 1 μM SAG and 1 μM TH for an additional 14 days. The mRNA expression was determined using RT-qPCR. The data are expressed as the mean ± SEM from four independent experiments.

(C) The effect of Cyc on mesoderm induction and subsequent osteoblast induction in mESCs. mESCs were cultured with 30 μM CHIR for 5 days in the presence or absence of 5 μM Cyc and treated for 14 days with SAG plus TH. The mRNA expression was determined using RT-qPCR on days 5 and 19, respectively. The data are expressed as the mean ± SEM from four independent experiments.

(D) A schematic showing the three-phase strategy for osteoblast differentiation from mESCs using the four small molecules under chemically defined conditions.

differentiate mesodermal cells into osteoblast precursors. Moreover, it also indicated that SAG alone might not be sufficient to direct the differentiation of these precursors into mature osteoblasts. In terms of molecules inducing osteoblast maturation, we identified the helioxanthin-derivative 4-(4-methoxyphenyl)pyrido[4′,3′:4,5]thieno[2,3-b]pyridine-2-carboxamide (TH) as an osteogenic small molecule that acts on preosteoblasts in a bone morphogenetic protein (BMP)-dependent manner (Ohba et al., 2007b). Furthermore, we recently reported the combinatorial effect of SAG and TH on the differentiation of mesenchymal cells into osteoblasts (Maeda et al., 2013).

Based on these findings, we hypothesized that pluripotent stem cells could be efficiently differentiated into osteoblasts under defined conditions by sequentially treating the cells with the above-mentioned small molecules in an appropriate manner. The present study was designed to establish a stepwise differentiation protocol for osteoblast differentiation from pluripotent stem cells by utilizing the small molecule inducers under serum-free and feeder-free conditions.

RESULTS AND DISCUSSION

We initially attempted to differentiate 2i-cultured mESCs into mesodermal cells by activating canonical Wnt signaling with CHIR in 2i culture media. CHIR upregulated the mesoderm-related genes *T* and *Mixl1* in a dose-dependent manner relative to day 0 (Figure 1A; Figure S1A available online). The expression of the pluripotency-related genes *Nanog*, *Pou5f1*, and *Sox2* was suppressed in cells treated with high concentrations of CHIR relative to day 0 (Figures 1A and S1A). In addition, the expression of

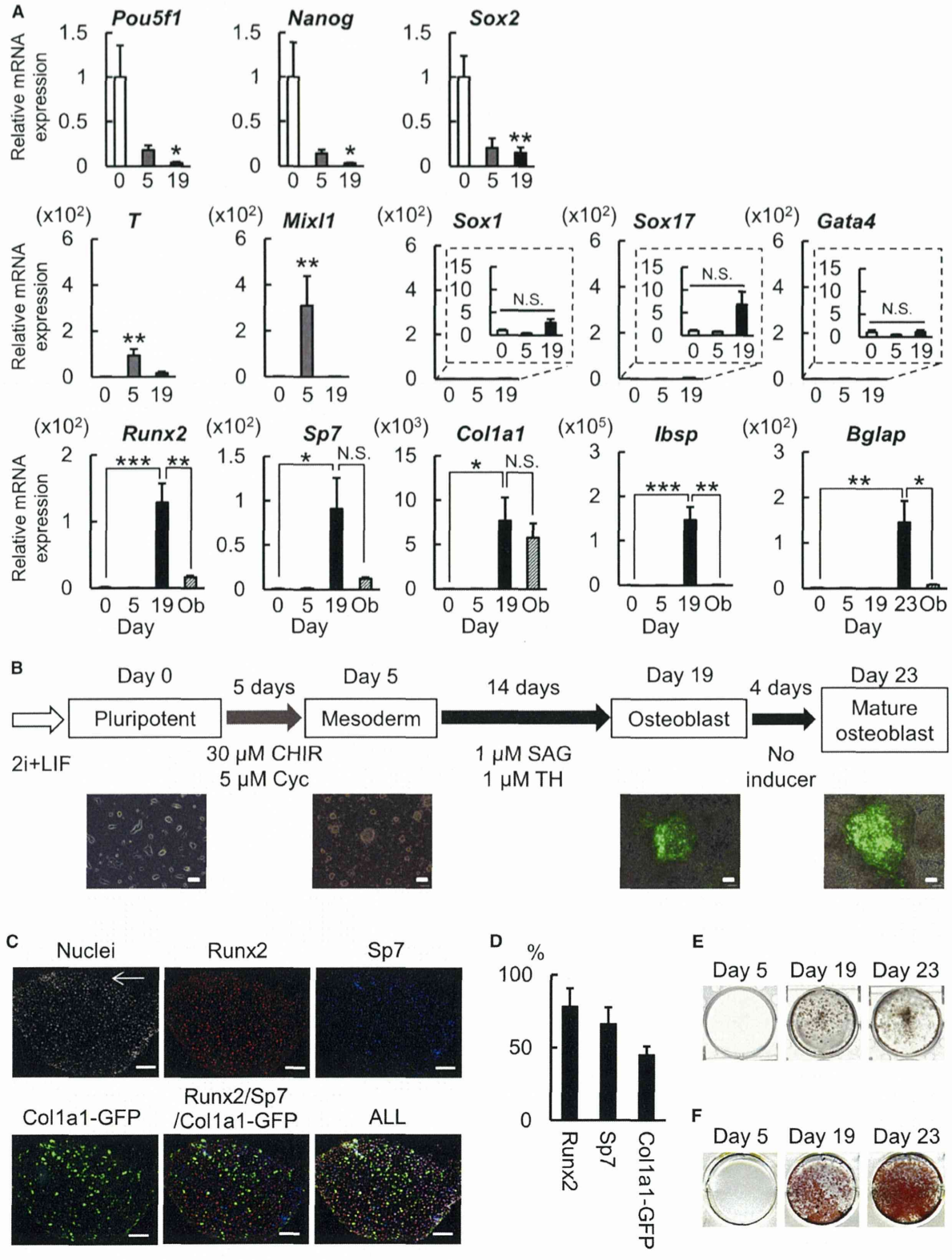

(legend on next page)

T was higher on day 5 than on day 7, and higher expression of the mesoderm-related genes was associated with higher expression of osteoblast-related genes in subsequent osteoblast induction (Figure S1B). Therefore, we selected the 5-day treatment protocol using 30 μM CHIR for the mesoderm induction of mESCs. To induce osteoblast differentiation of the mESC-derived mesoderm cells, we then cultured them in 2i culture media containing 1 μM SAG, 1 μM TH, and other osteogenic supplements (Jaiswal et al., 1997). *Runx2*, *Sp7*, and *Ibsp* were upregulated following treatment for 2 weeks with SAG plus TH relative to the control group (Figure 1B). Thus, the stepwise differentiation from mESCs into osteoblasts via mesoderm formation was achieved using the three small molecules CHIR, SAG, and TH.

Given the roles of Hh signaling during the development of the CNS (Martí and Bovolenta, 2002), recombinant Hh proteins or SAGs have been used to differentiate pluripotent stem cells into motor neurons (Nizzardo et al., 2010). Moreover, 2i-cultured ESCs preferentially differentiate into ectoderm lineages rather than mesoderm lineages (Marks et al., 2012). These findings led us to examine whether the suppression of Hh signaling during the mesoderm induction would block neuro-ectoderm specification, resulting in enhanced osteoblast differentiation. The combinatorial use of the Hh signaling inhibitor cyclopamine (Cyc) and CHIR during the 5-day mesoderm induction induced the downregulation of *Sox1* on day 5 and led to increased osteoblast differentiation (Figure 1C).

As shown in Figure 1D, we propose an optimized strategy for promoting osteoblast differentiation from mESCs under chemically defined conditions. This strategy consists of three phases: the maintenance of mESCs using 2i plus leukemia inhibitory factor (LIF) culture, mesoderm induction by CHIR in combination with Cyc-mediated suppression of neuro-ectoderm differentiation, and osteoblast induction by SAG and TH. Given that Cyc induces SMO translocation to the primary cilium despite its inhibitory effect on Hh signaling (Wang et al., 2009), the accumulated SMO in the cilium may result in increased sensitivity to subsequent SAG treatment, which may also contribute to the osteoblast differentiation by SAG and TH during the osteoblast induction phase. SAG and TH cooperatively induce osteoblast differentiation, possibly through SAG-mediated specification into an osteoblast lineage and TH-mediated promotion of late osteoblast differentiation (Hojo et al., 2013; Maeda et al., 2013; Ohba et al., 2007b).

Gene expression patterns in mESCs cultured according to this strategy are shown in Figure 2A. *Pou5f1*, *Nanog*, and *Sox2* were significantly downregulated on day 19, indicating that the mESCs gradually exited from the pluripotent state as differentiation progressed. *T* and *Mixl1* were upregulated by mesoderm induction (day 5) and in turn were downregulated by osteoblast induction (day 19). *Sox1*, *Sox17*, and *Gata4*, which are ectoderm and endoderm marker genes, were not altered throughout the culture. These data suggested that the present strategy specifically directs pluripotent cells toward a mesodermal cell fate. The osteoblast-related genes, *Runx2*, *Sp7*, *Col1a1*, and *Ibsp*, were upregulated during the osteoblast induction phase (day 19) relative to day 0; *Runx2*, *Sp7*, *Col1a1*, and *Ibsp* were upregulated approximately 128-, 91-, 7,680-, and 147,300-fold, respectively. However, the 19-day culture was not long enough for the cells to express *Bglap*, a bona fide marker of mature osteoblasts; culturing the cells for an additional 4 days in the absence of SAG or TH induced a 145-fold upregulation of *Bglap*.

Expressions of the osteoblast-related genes in the induced cells were higher than or comparable to those in cultured mouse primary osteoblasts (Figure 2A). Expressions of osteoblast-related transcription factors in the induced cells were comparable to those in freshly isolated mouse osteoblasts (fresh mObs), although the expressions of matrix genes in the induced cells were not as high as those in the fresh mObs (Figure S2A). When gene expressions were compared between the present strategy and an

Figure 2. Characterization of mESC-Derived Cells Generated Using the Present Strategy for Osteoblast Differentiation

(A) Expressions of pluripotency-related (*Pou5f1*, *Nanog*, and *Sox2*), mesoderm-related (*T* and *Mixl1*), ectoderm-related (*Sox1*), endoderm-related (*Sox17* and *Gata4*), and osteoblast-related genes (*Runx2*, *Sp7*, *Col1a1*, *Ibsp*, and *Bglap*) on days 0 (white bars), 5 (gray bars), 19, and 23 (black bars) and cultured calvarial osteoblasts isolated from mouse neonates (Ob; hatched bars). The *Sox1*, *Sox17*, and *Gata4* expression data are shown in the dotted rectangular box with the smaller scale of the y axis. The data are expressed as the mean ± SEM from eight independent experiments. *$p < 0.05$ versus day 0; **$p < 0.01$ versus day 0; ***$p < 0.001$ versus day 0; N.S., nonsignificant versus day 0. See also Figures S2A–S2C.

(B) A schematic showing the four-phase strategy for directing mESCs into mature osteoblasts. The lower panels indicate the morphology and expression of GFP in 2.3 kb Col1a1-GFP mESCs cultured according to the present strategy. Scale bars, 100 μm.

(C) Protein expressions of the osteoblast-related markers in 2.3 kb Col1a1-GFP mESCs cultured according to the present strategy on day 19. The arrow shows the surface of the cell cluster. Scale bars, 100 μm. Nuclei and SP7 are shown in pseudocolor. See also Figure S2D.

(D) Quantification of cells expressing osteoblast-related marker proteins. The data are expressed as the mean of percentages of cells positive for both DAPI and markers in total of DAPI-positive cells analyzed ± SEM from three independent experiments.

(E and F) von Kossa staining (E) and alizarin red staining (F) on days 5, 19, and 23 in mESCs cultured according to the present strategy.

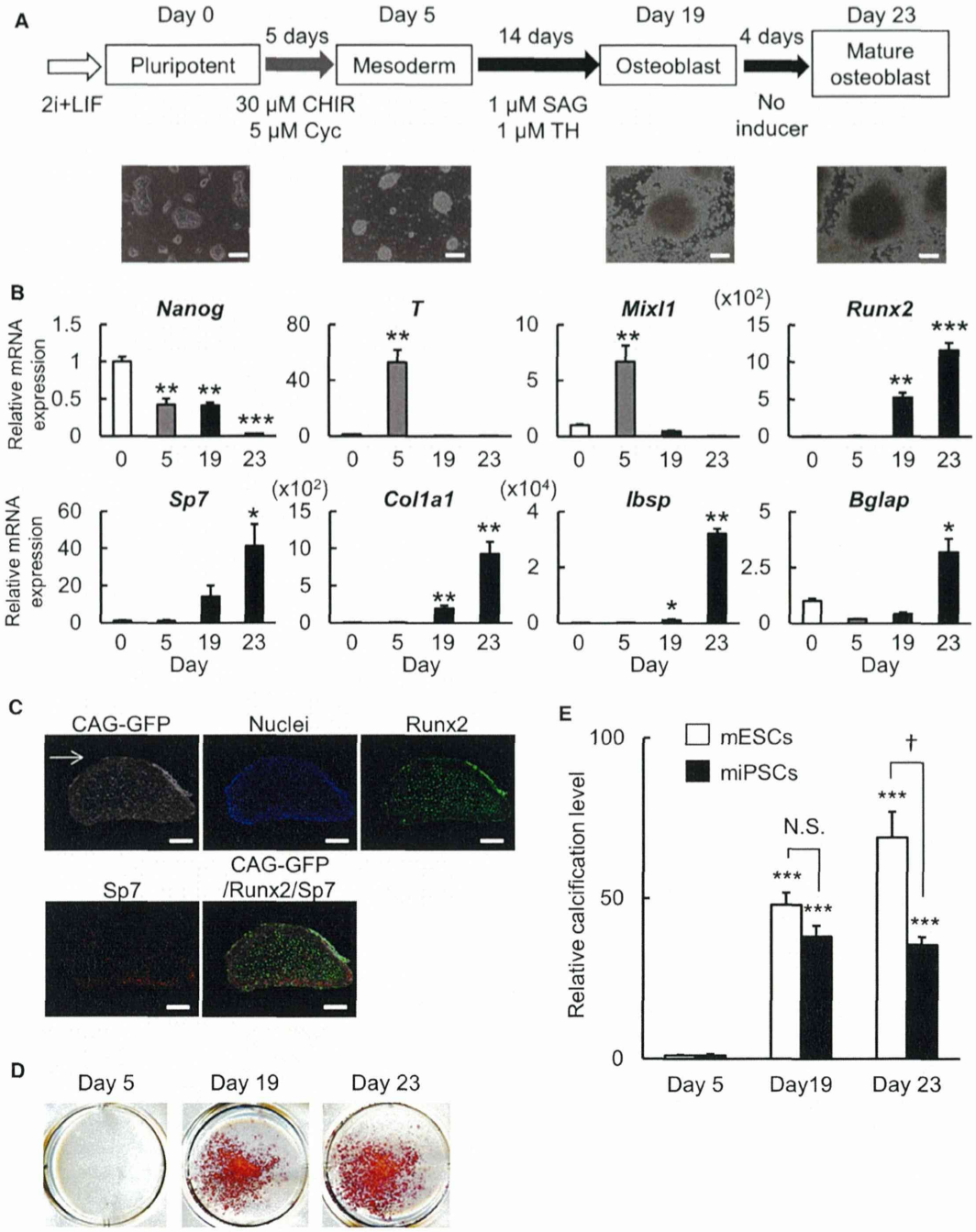

Figure 3. Differentiation of miPSCs into Osteoblasts

(A) A schematic showing the strategy for inducing osteoblast differentiation of miPSCs. The lower panels show the morphology of colonies of miPSCs and induced cells on days 0, 5, 19, and 23. Scale bars, 100 μm.

(B) Expressions of pluripotency-related (*Nanog*), mesoderm-related (*T* and *Mixl1*), and osteoblast-related genes (*Runx2*, *Sp7*, *Col1a1*, *Ibsp*, and *Bglap*) on days 0 (white bars), 5 (gray bars), 19, and 23 (black bars) in miPSCs. The data are expressed as the mean ± SEM from six independent experiments. *$p < 0.05$ versus day 0; **$p < 0.01$ versus day 0; ***$p < 0.001$ versus day 0.

(C) Protein expressions of the osteoblast-related markers in CAG-GFP miPSCs cultured according to the present strategy on day 23. RUNX2, SP7, and GFP are shown in pseudocolor. The arrow shows the surface of the cell cluster. Scale bars, 100 μm.

(legend continued on next page)

EB-based conventional one (Kawaguchi et al., 2005), the present strategy induced significantly lower expressions of *Sox17* and *Gata4* on day 19 and higher expressions of *Runx2*, *Sp7*, *Col1a1*, *Ibsp*, and *Bglap* on day 19 or 23 than the conventional method (Figure S2B). The present strategy is likely to differentiate mESCs into an osteoblast lineage more specifically than the conventional method, at least partly by avoiding their differentiation into unfavorable lineages. When we examined gene expressions at several time points during the culture (Figure S2C), the expression profile resembled a proposed model for the Hh signaling-mediated specification of skeletal progenitors into *Runx2*-positive osteoblast precursors and their subsequent differentiation into osteoblasts in skeletal development (Rodda and McMahon, 2006).

Thus, we established a strategy to direct mESCs toward a mature osteoblast cell fate by sequentially using four small molecules, CHIR, Cyc, SAG, and TH, under chemically defined conditions. This protocol involves the addition of a fourth osteoblast maturation phase to the three-phase strategy described earlier (Figure 2B). The effectiveness of the strategy was further confirmed by the expression of GFP on days 19 and 23 in mESCs engineered to express GFP under the control of an osteoblast-specific rat 2.3 kb *Col1a1* promoter (2.3 kb Col1a1-GFP mESCs) (Figure 2B) (Ohba et al., 2007a).

We used immunohistochemistry to measure the expression of RUNX2, SP7, and GFP in the induced 2.3 kb Col1a1-GFP mESCs. RUNX2, SP7, and the 2.3 kb Col1a1-GFP were highly expressed in the induced cells on day 19. RUNX2 and SP7 were colocalized in nuclei, and 2.3 kb Col1a1-GFP was largely observed in the cytoplasm and nuclei (Figure 2C). The average percentages of RUNX2-, SP7-, and GFP-positive cells were 78% ± 3%, 66% ± 5%, and 45% ± 1%, respectively (Figure 2D). The different percentages of those markers in our culture are consistent with the physiological process of osteoblast development. The percentages enable us to estimate the final yields of each osteoblastic population, given that 900,000 ± 150,000 cells/cm^2 were obtained on day 19 of the culture from 100,000 cells/cm^2 of input. Pluripotency markers were hardly expressed in the induced cells on day 19 (Figure S2D). The average percentages of OCT4-, NANOG-, and SOX2-positive cells were 2.3% ± 0.6%, 1.5% ± 0.7%, and 9.0% ± 3.1%, respectively (Figure S2D). In addition, BRACHYURY (T), a mesoderm maker, was ubiquitously expressed in the induced cells on day 5 (Figure S1C). von Kossa staining and alizarin red staining revealed the uniform formation of calcified cell clusters by days 19 and 23 (Figures 2E and 2F). These results indicate that the present strategy induced both the expression of osteoblast-related genes and the calcification of matrix, two key features of osteoblasts.

To confirm that the present strategy could be useful for investigating osteoblast development using gene-manipulated mESCs in vitro, we examined whether *Runx2*$^{-/-}$ mESCs cultured using the present strategy could molecularly recapitulate osteoblast phenotypes in *Runx2*$^{-/-}$ mice (Figure S3A). *Runx2*$^{-/-}$ mESCs showed similar transient upregulation of *T* to *Runx2*$^{+/+}$ mESCs, but *Sp7* and *Bglap* were hardly upregulated in *Runx2*$^{-/-}$ mESCs on day 19 compared to day 0 and day 5. Importantly, the expression of the early osteoblast marker gene *Ibsp* showed a 212-fold upregulation in *Runx2*$^{-/-}$ mESCs on day 19, although the level was lower than that observed in *Runx2*$^{+/+}$ mESCs. In alizarin red staining, the calcification level of *Runx2*$^{-/-}$ mESCs was lower than that of *Runx2*$^{+/+}$ ones on both days 19 and 23 (Figures 2F, S3B, and S3C). These observations were consistent with the bone phenotypes of *Runx2*$^{-/-}$ mice (Komori et al., 1997; Tu et al., 2012). Thus, the present strategy can at least partially recapitulate physiological osteoblast development and will be useful for analyzing osteoblast development using gene-manipulated ESCs in vitro.

Because the direct differentiation of mouse iPSCs (miPSCs) and human iPSCs (hiPSCs) into osteogenic cells has been previously reported by Bilousova et al. (2011), Kao et al. (2010), and Levi et al. (2012), we applied the present strategy to 2i-adapted miPSCs established from fibroblasts of mice expressing GFP (CAG-GFP miPSCs) (Okabe et al., 1997) (Figure 3A). *Nanog* was downregulated throughout the culture compared to day 0. *T* and *Mixl1* were transiently upregulated by mesoderm induction on day 5. The osteoblast-related genes *Runx2*, *Sp7*, *Col1a1*, *Ibsp*, and *Bglap* were upregulated by the osteoblast induction (Figure 3B). RUNX2 and SP7 proteins were highly expressed in the induced cells on day 23, and their signals were merged with that of GFP (Figure 3C), suggesting that CAG-GFP miPSCs were differentiated into cells expressing osteoblast-related proteins. Calcified cell clusters were formed on days 19 and 23 (Figure 3D). In the comparison of calcification levels between mESCs and miPSCs, both cell types were calcified at a similar level on day 19; mESCs then showed more calcification on day 23 (Figure 3E).

(D) Alizarin red staining on days 5, 19, and 23 in miPSCs cultured according to the present strategy.
(E) Alizarin red staining-based quantification of calcification levels in mESCs and miPSCs cultured according to the present strategy, relative to day 5 in each cell type. ***$p < 0.001$ versus day 5 in each cell type; N.S., nonsignificant; †$p < 0.05$. The data are expressed as the mean ± SEM from six independent experiments.

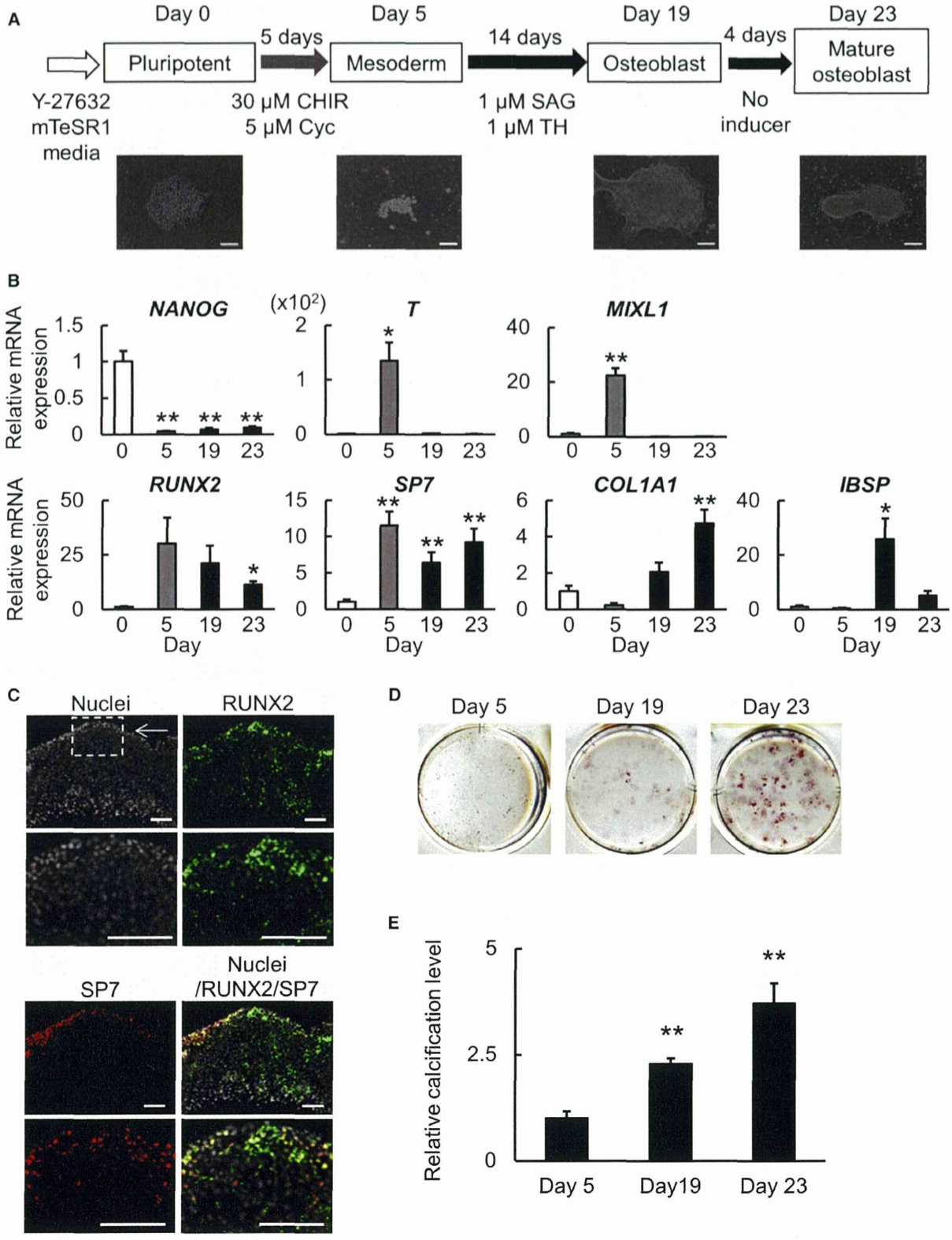

(legend on next page)